Fluid Dynamics Transactions, Vol. 4, pp. 619–633
Institute of Fundamental Technical Research, Polish Academy of Sci., Warsaw

DISINTEGRATION OF A LIQUID SHEET DUE TO GRAVITY FORCE

R. PUZYREWSKI (GDAŃSK) and E. E. ZUKOSKI (PASADENA – CALIFORNIA)

An experimental study was made of the disintegration of a liquid sheet due to gravity force. The influence of surface tension, viscosity, and density of liquids on the phenomenon of disintegration was found. Conditions of liquid sheet breaking into streams, as well as the frequency of appearance of streams and the mean diameter of droplets independent of properties of the liquid, were found experimentally.

1. Introduction

The problem studied in this paper concerns the disintegration of a liquid sheet falling under gravitational force. The sheet in question here is that formed when liquid, flowing down a vertical plate, leaves the plate at its bottom edge. In this problem, surface tension, together with viscous, inertial, and gravitational forces appear to be important.

The disruption of liquid sheets, films, and droplets has been extensively studied—e.g., RAYLEIGH, TAYLOR, DODD and BUZUKOW—and the present study is the result of the interest in the formation of droplets in steam turbines. When the steam flowing through a turbine becomes wet, the blade surfaces are covered with a thin sheet of water which drains to the edge of the blade and which is torn off the blade by aerodynamic forces in relatively large droplets. This problem has been studied in some simple experiments by R. PUZYREWSKI and S. KRZECZKOWSKI.

The relationships which describe the steady motion of a thin fluid film falling along a vertical plate under the influence of gravity are well known—e.g. LEVITCH—and the new material discussed here concerns the disintegration of such a film at the bottom edge of the plate. In all the cases studied, the sheet covered the entire plate, and gravitational and viscous forces were in equilibrium on the plate. The influences of surface tension, viscosity, and density on the disintegration processes were studied and the conditions under which the sheet is disrupted, the number of streams formed and their spacing, and the diameter of droplets formed at low flow rates were found experimentally.

2. Description of the Stand

The sketch of the stand is given in Fig. 1. The liquid flowed through the small gap in the calibrating box and covered the flat plate. The position of the camera and also the source of the light is shown in the sketch. During the experiments, the dimensions of

the gap were varied between 0.005 and 0.3 cm. In addition, the shape of the bottom edge of the plate was changed; the three shapes used are shown in Fig. 2.

The fluids used in the experiments were tap water, carbon tetrachloride, ethyl alcohol, glycerine, and a mixture of the two last named with water. The properties of these liquids

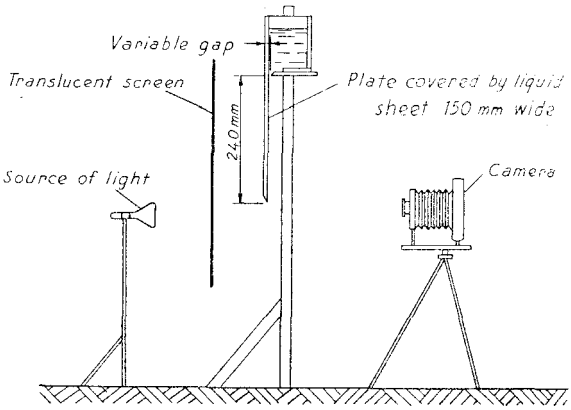

FIG. 1.

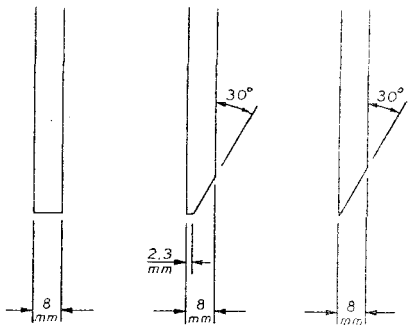

FIG. 2.

are given in Table 1. The viscosity of the liquids was measured on a Hoeppler viscosimeter and the rest of the parameters were taken from values given in the Handbook of Chemistry and Physics.

Table 1

No	Liquid	Density ϱ g/cm^3	Viscosity ν_2 cm^2/sec	Surface Tension, g/sec^2	Remarks
1	glycerine	1.25	$436 \cdot 10^{-2}$	64	not pure glycerine
2	mixture, glycerine and water	1.24	$283 \cdot 10^{-2}$	65	93% glycerine*
3	,,	1.233	$155 \cdot 10^{-2}$	65	90% glycerine*
4	,,	1.215	$65 \cdot 10^{-2}$	66.5	84% glycerine*
5	,,	1.19	$23.3 \cdot 10^{-2}$	67	74% glycerine*
6	,,	1.17	$8.56 \cdot 10^{-2}$	67	60% glycerine*
7	,,	1.16	$4.35 \cdot 10^{-2}$	72	45% glycerine*
8	,,	1.074	$2.16 \cdot 10^{-2}$	72	30% glycerine*
9	ethyl alcohol	0.79	$1.45 \cdot 10^{-2}$	21.5	chemically pure
10	mixture, ethyl alcohol and water	0.984	$1.476 \cdot 10^{-2}$	46	10% ethyl alcohol+
11	,,	0.9719	$1.756 \cdot 10^{-2}$	38	18% ethyl alcohol+
12	carbon tetrachloride	1.585	$0.662 \cdot 10^{-2}$	26.8	chemically pure
13	water	1	$1 \cdot 10^{-2}$	72.75	Pasadena city water

* by volume + by weight

3. General Description of Phenomena

Before discussing in detail some of the phenomena which occur at the downstream edge of a vertical plate on which a liquid stream is flowing, it is desirable to give a general picture of such phenomena as a whole. Consider an experiment in which the fluid flow rate is allowed to change from a very large value to zero. At high flow rates, a solid sheet of fluid leaves the plate and remains undisturbed, except for edge effects, for some distance downstream of the plate. As the flow decreases, a critical rate is reached at which the sheet becomes unstable and breaks up into a small number of distinct streams with their origins at the edge of the plate. For a small range of flow rates, the number of streams increases rapidly with decreasing flow rate and then remains constant for a large range of flow rates. At the lower end of this flow range, the flow from the edge of the plate is reduced to the point at which the fluid merely drips from the plate. However, the number of points from which the fluid drips is still almost equal to that from which distinct streams flowed off the plate. Finally, if the flow is reduced sufficiently, most of these points "dry up" and only a few drip positions remains. The range of phenomena described here is illustrated in Figs. 3, 4, and 5.

In Fig. 3 the influence of flow rate is shown for three fluids. Figure 3a shows the continuous sheet strongly influenced by surface tension effects at the edges in the case of glycerine and less so for alcohol and water. In the case of alcohol and water, the transition to the constant number of streams is shown in 3a and 3c, and finally the lower end of the flow range in which the number of drip points is constant is shown in Fig. 3d for four fluids. The length separating the number of points from which the fluid leaves the plate, λ, is shown for water in Fig. 4 as a function of the flow rate divided by the critical value, Q/Q_{cr}.

At high flow rates, waves were observed in the fluid on the plate. These waves were not two dimensional, but did move down the plate at a roughly uniform speed. This phenomenon is illustrated by the three consecutive photographs shown in Fig. 5. The waves are apparently the well-known roll waves—e.g., LEVITCH. The wave speed compared to the mean fluid flow speed was observed to be 2.94, whereas the expected value for roll waves is 3.0. According to LEVITCH, the waves should appear when the mean flow Reynolds number $Q/\varrho\nu$ is 30; the limit observed in the present work was about 20. The waves appeared to have no influence on the phenomenon observed at the lip of the plate, which is the subject of the present paper.

Several features of the flow described above were sufficiently regular to warrant investigation. There were: (1) the value of the flow rate, Q, at which the continuous sheet breaks up, called the critical flow rate, Q_{cr}; (2) the shape of the edge of the solid sheet for flow rates greater than the critical value; (3) the wave length λ separating the sites at which material leaves the plate, for the intermediate flow rates; and finally (4) the mean value of droplet radius a which dripped from the plate, at low flow rates. Values of Q_{cr}, λ, and a were obtained for a variety of fluids and for as wide a range of flow rates as possible.

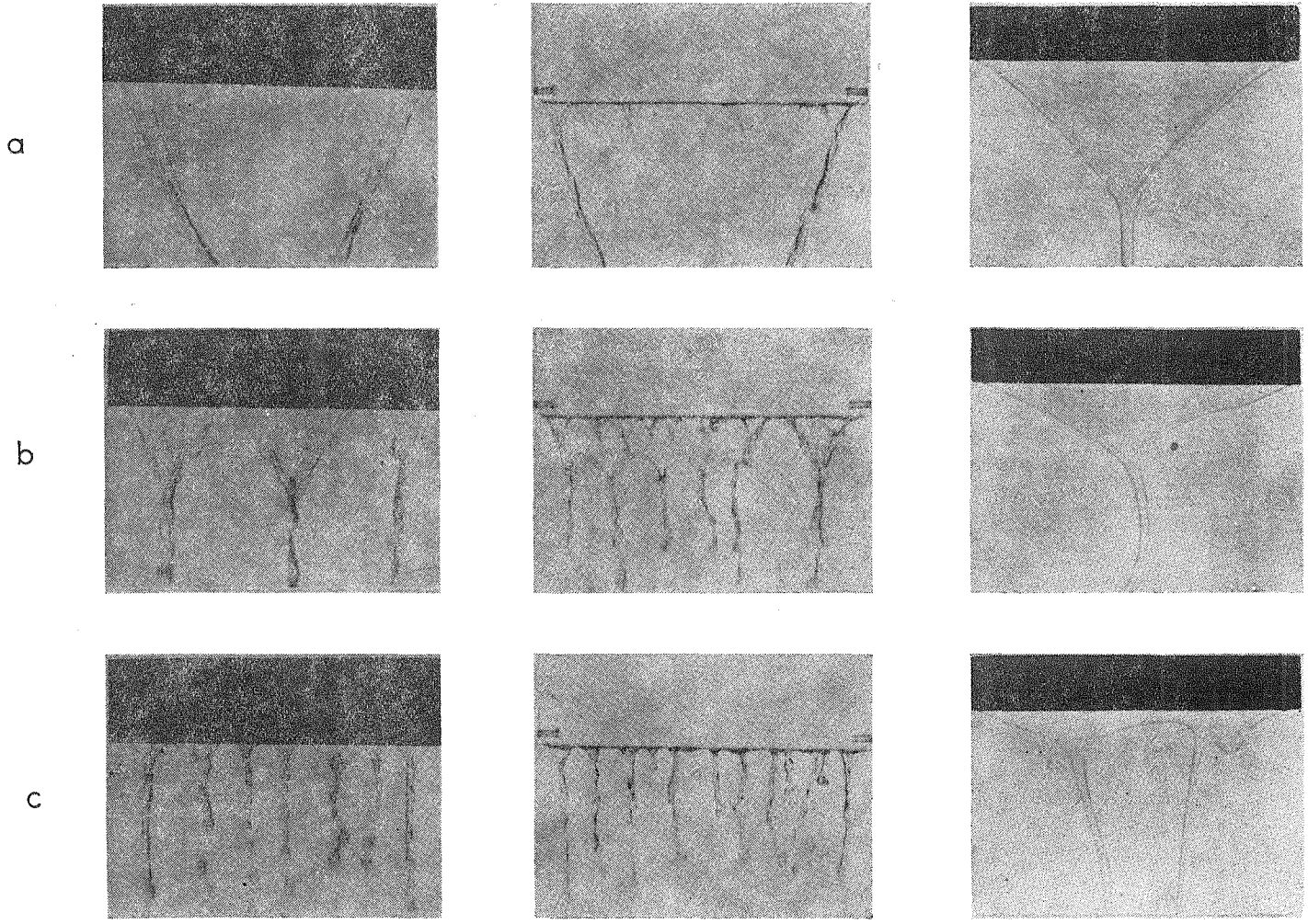

FIG. 3a, b, c.

FIG. 3d.

4. Critical Flow Rate

Although the breakup of the continuous sheet, described above, occurred for all fluids tested, there were differences between the breakup obtained with low viscosity fluids and with high viscosity fluids. These differences are illustrated by comparing Figs. 3a and 3b for water and alcohol with Figs. 3a, 3b, and 3c for glycerine. The glycerine sheet was always smooth in appearance, and the onset of sheet disruption occurred when the

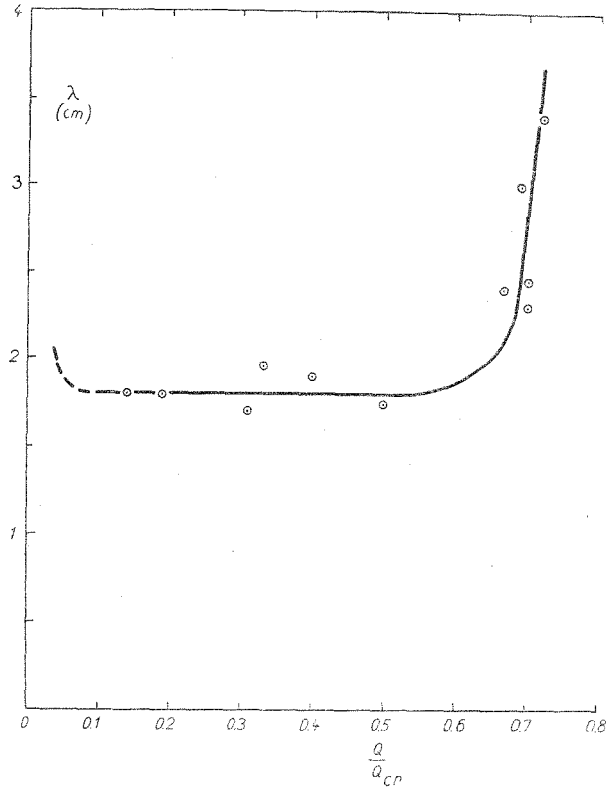

FIG. 4.

angle made by the edges of the sheet with the edge of the plate was quite small. An oscillation in the position of the edge of the sheet, (e.g., Figs. 3b and 3c) then led to the disruption of the film. For water and alcohol, the sheet was more rough in appearance, and the sheet disruption was marked by the irregular appearance of holes in the body of the sheet. However, in both cases, the disruptions were stabilized by the edge of the plate and became attached there.

The critical flow rate was independent of the influence of end plates and of the original thickness of the film, provided that the wall velocity profile was well developed.

One of the difficulties in studying the disruption of the film is that some of the flow parameters of interest—e.g. the film thickness h and mean flow speed of the film $\bar{u}$ at

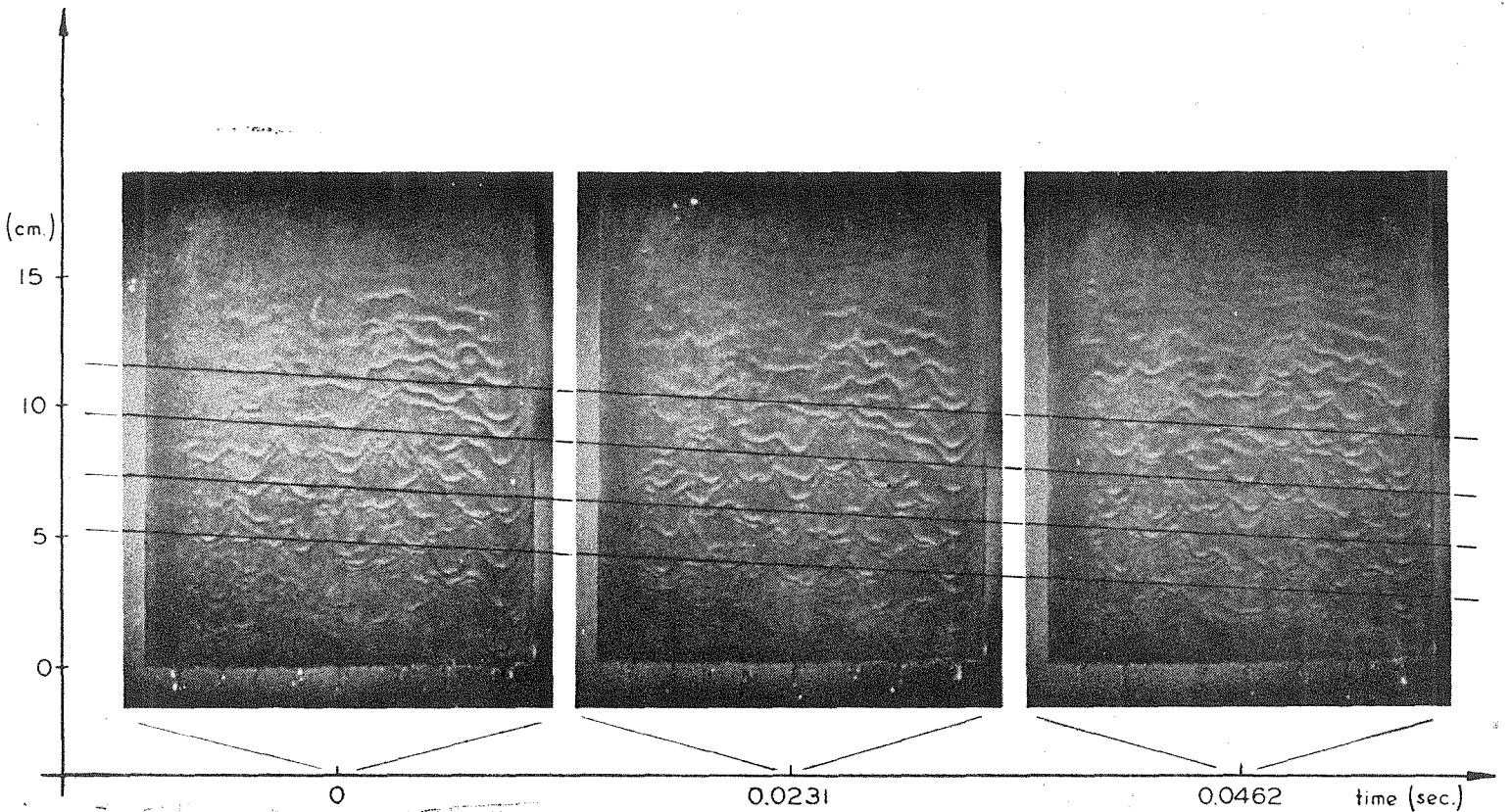

WATER Re = 80

FIG. 5.

the edge of the plate—are also strong functions of the fluid properties and gravitational acceleration g:

$$h = \frac{Q}{\varrho \bar{u}}, \qquad \bar{u} = \frac{gh^2}{3\nu}. \tag{4.1}$$

Hence, these parameters cannot be changed independently of the fluid properties, and the determination of the properties which are pre-dominant in fixing the film disruption is made difficult. For this reason, a straightforward dimensional analysis was made in which the critical flow rate Q_{cr} was assumed to depend on ν, σ, ϱ and g;

$$Q_{cr} = f(\nu, \sigma, \varrho, g). \tag{4.2}$$

For this set of parameters, only one non-dimensional group could be obtained for the argument of f:

$$\nu \sqrt[4]{\left(\frac{\varrho}{\sigma}\right)^3 g} \equiv \frac{1}{m}. \tag{4.3}$$

Among only three combinations of arguments which have the dimension of a mass flow rate per unit length, $\varrho\nu$ was chosen to normalize Q_{cr}. Finally, equation (4.2) in non-dimensional form is

$$Q_{cr}/\varrho\nu = f(m). \tag{4.4}$$

It is interesting to note that

$$\frac{Q_{cr}}{\varrho\nu} = \mathrm{Re}_{cr} \tag{4.5}$$

whereas

$$m = \frac{\mathrm{Re}_{cr}\,\mathrm{We}^{3/4}}{\mathrm{Fr}^{1/2}} \tag{4.6}$$

where the Reynolds, Froude, and modified Weber numbers are definite, as

$$\mathrm{Re}_{cr} = \frac{\bar{u}h}{\nu}, \qquad \mathrm{Fr} = \frac{\bar{u}^2}{gh}, \qquad \mathrm{We} = \frac{\sigma}{\varrho g h^2}. \tag{4.7}$$

Results of the experimental measurements are given in Tabele 2 and in Fig. 6, in which Re_{cr} is plotted versus m with logarithmic scales.

The points on this graph lie along the straight line

$$\mathrm{Re}_{cr} = 0.266\, m^{1.176} \tag{4.8}$$

The equation for the correlation, shown in Fig. 6, can be rewritten in terms of the mean speed and film thickness by means of Eqs. (4.1). This can be done in such a way that the dependence on the Reynolds number, $Q_{cr}/\varrho\nu = u_{cr}h_{cr}/\nu$ is made relatively weak. For example,

$$\frac{Q_{cr}}{\sigma/\sqrt{gh_{cr}}} = 0.268\,\mathrm{Re}^{0.033}. \tag{4.9}$$

Unfortunately, other forms are also possible, and because of the interrelationship between u, h, Q and ν, no definitive form of the results which pertain to the disruption of an arbitrary sheet can be deduced from these experiments.

The simple calculation based on the balance between surface tension force $2\cdot\sigma\cdot 1$ and aerodynamic pressure force $\frac{\varrho\bar{u}^2}{2}h\cdot 1$ gives a relation slightly different from (4.8).

Solving two equations

$$2\sigma = \frac{\varrho\bar{u}^2}{2}h \quad \text{and} \quad Q = \frac{\varrho g h^3}{3\nu} \tag{4.10}$$

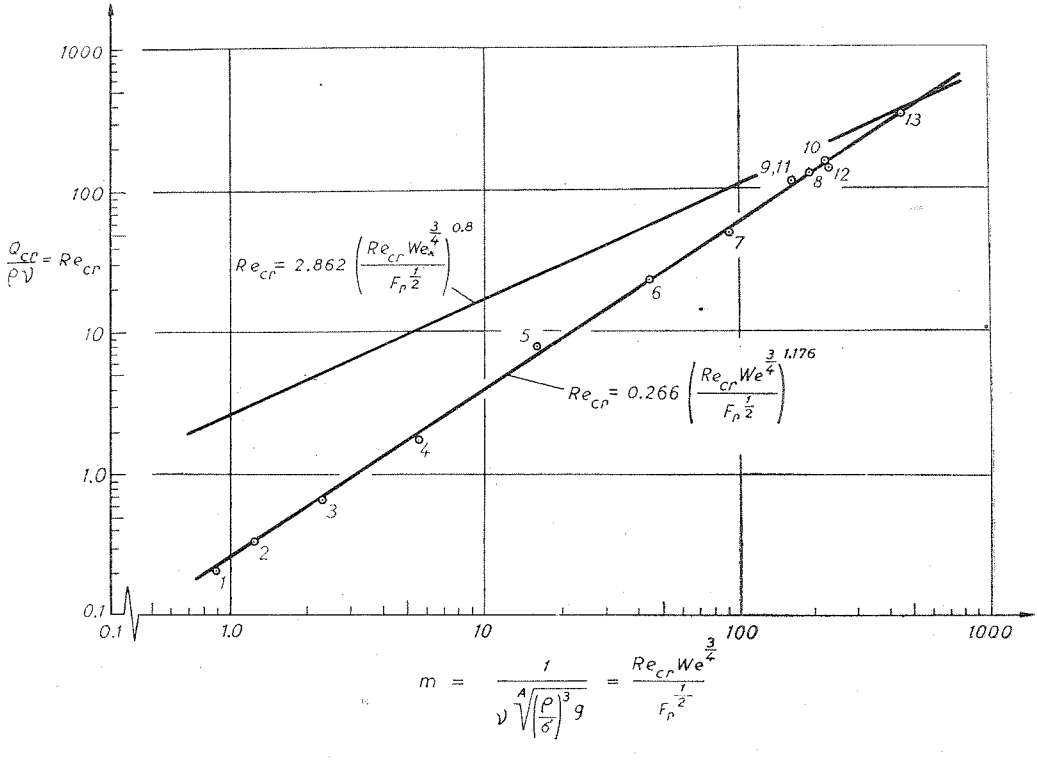

FIG. 6.

for $\mathrm{Re} = \frac{\varrho\bar{u}h}{\varrho\nu}$, we obtain

$$\mathrm{Re}_{cr} = 2.862\, m^{0.8} \tag{4.11}$$

This line as it is shown on the Fig. 6 lies higher than experimental points. Equation (4.11) gives more satisfactory results for higher values of m.

5. Geometry of Sheet Edge

The shape of the sheet obtained in the experiments for flow rates above Q_{cr} was strongly influenced by the surface tension forces acting on the edges of the sheet, (see Fig. 3). A simple model for the flow was developed which enables a calculation of the shape of the edge of this sheet. The sketch of the flow presented in Fig. 7 shows the principal

features of the flow used in discussing the model, which is based on a simple momentum balance and on the experimental fact that the streamlines in the flow downstream of the plate go straight down to the edge of the liquid sheet.

Table 2

No. (as in Table 1)	Q_{cr} / $\frac{g}{cm \cdot s}$	Re_{cr}	$\frac{1}{v\sqrt[4]{\left(\frac{\varrho}{\sigma}\right)^3 g}}$
1	1.105	0.202	0.785
2	1.1	0.319	1.23
3	1.285	0.67	2.26
4	1.35	1.71	5.53
5	2.09	7.55	15.78
6	2.19	22.26	44.0
7	2.495	49.5	91.0
8	2.98	128.0	194.0
9	1.32	115.0	160.5
10	2.18	150.0	217.0
11	1.93	113.0	162.0
12	1.42	135.0	225.0
13	3.33	333.	444.0

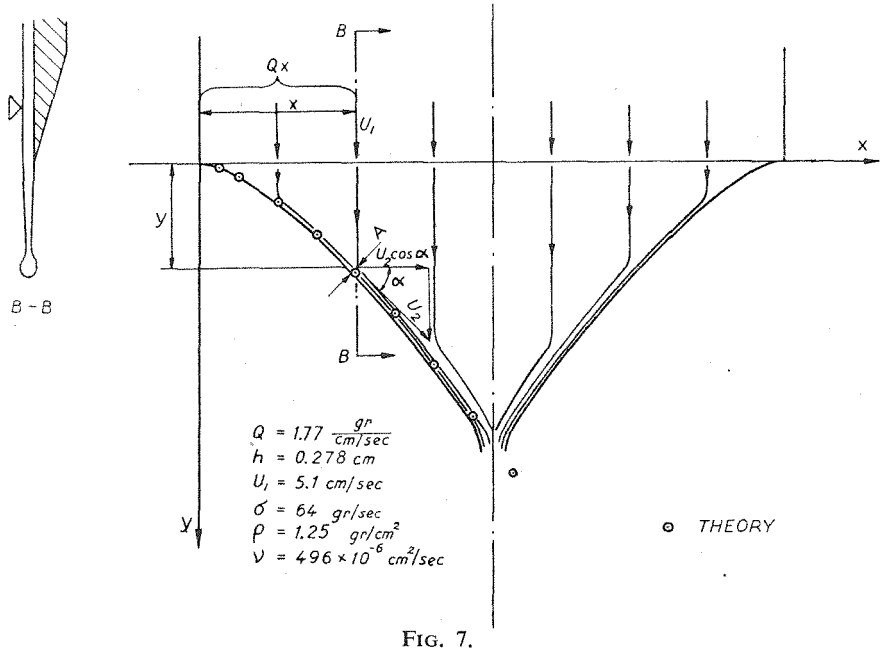

FIG. 7.

In this case, conservation of mass gives the mass flow through the cross section at A to be Qx. Then we can write the equation of momentum in the x-direction for the triangularshaped section of the sheet below the edge and to the left of the section $B-B$. If

one takes into account the surface tension force along the streamline and the x-component of momentum flux which makes contribution only at the edge of the sheet at A, the momentum balance is:

$$Qxu_2\cos\alpha = 2\sigma y, \tag{5.1}$$

where

$$\tan\alpha = \frac{dy}{dx} \tag{5.2}$$

and from Bernoulli's equation,

$$u_2 = \sqrt{u_1^2+2gy}, \tag{5.3}$$

where u_1 is given by Eq. (4.6).

Combination of these equations gives a non-linear differential equation for the sheet shape below the edge of the plate:

$$y^2\left(\frac{dy}{dx}\right)^2 + y^2 - x^2(A+By) = 0, \tag{5.4}$$

where

$$A = \frac{1}{4\sqrt[3]{9}}\sqrt[3]{\frac{g^2}{\sigma^2\varrho^4\nu^2}}\,Q^{\frac{10}{3}} \tag{5.5}$$

and

$$B = \frac{1}{2}\frac{g}{\sigma^2}Q^2. \tag{5.6}$$

The initial condition is

$$y = 0 \quad \text{for} \quad x = 0.$$

Using a polynomial expansion near the zero of the form:

$$y = a_1 x + a_2 x^2 + a_3 x^3 + \ldots. \tag{5.7}$$

we get

$$a_1 = \sqrt{\frac{\sqrt{1+4A}-1}{2}}, \tag{5.8}$$

$$a_2 = \frac{B}{6a_1^2+2}, \tag{5.9}$$

$$a_3 = \frac{Ba^2 - a_2^2(1+13a_1^2)}{a_2(8a_2^2+2)} \tag{5.10}$$

and so forth.

For very large x, the asymptotic solution obtained by F. E. MARBLE is

$$y = \left(\frac{4}{3}B^{\frac{1}{2}}x^2\right)^{\frac{2}{3}}. \tag{5.11}$$

The results of the numerical solution for small x are shown in Fig. 7. The agreement with the real shape is good except in the neighbourhood of the center line, where, as might be expected, the two streams meet and the liquid falls vertically.

6. Frequency of Appearance of Streams and Mean Diameter of Droplets

For Reynolds numbers less than about 0.7 Q_{cr}, regularity was observed in the spacing of the streams leaving the edge, and this regularity extended to the lowest flow rates for which steady state measurements could be made.

The dependence of the average spacing λ on flow rate is shown in Fig. 4. In the region where λ is independent of flow rate, it seems reasonable that only the relation between surface tension force and gravity force governs this phenomenon. The dimensional analysis approach gives the formula

$$\lambda = f(\sigma, \varrho, g) = C_1 \sqrt{\frac{\sigma}{\varrho g}} \tag{6.1}$$

and the experimental results given in Fig. 8 show good agreement with this equation. The slope of the lines on this graph determines the magnitude of the constant and gives a value of about $C_1 = 6.8$.

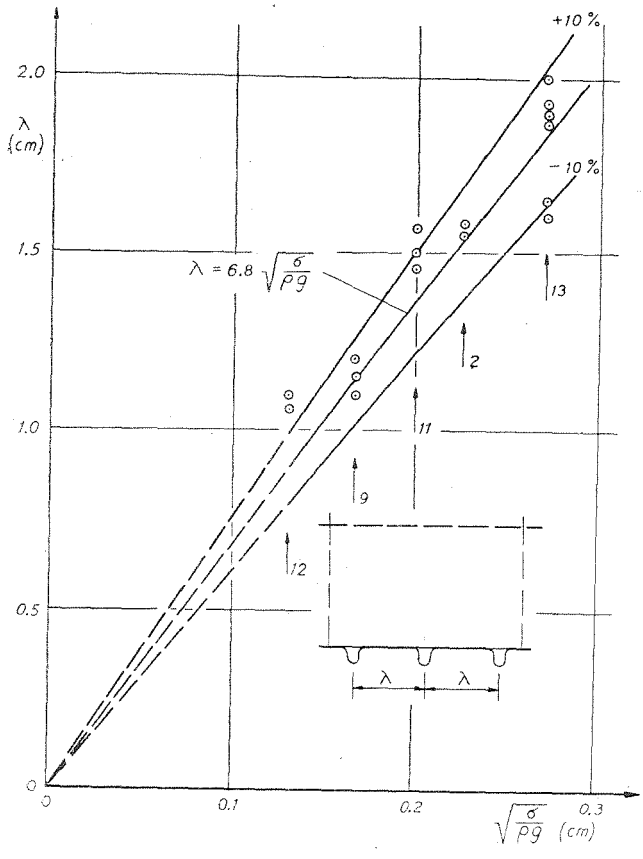

FIG. 8.

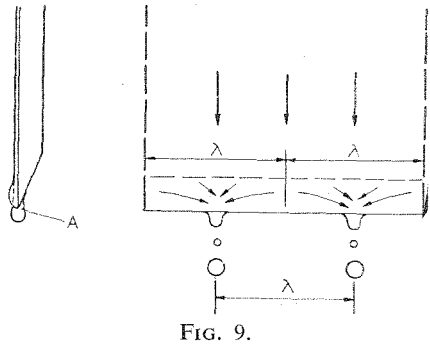

FIG. 9.

The phenomena responsible for the regular spacing observed of the fluid streams appear to be as follows. When fluid first reaches the edge of the plate, a liquid rampart is formed—e.g., Fig. 9, point A. The gravitational force on the fluid rampart is supported by surface tension forces between the liquid and the plate until the liquid film thickness is greater than a certain critical value. When this dimension is exceeded, due to flow down the plate, this point becomes a source for droplets. In the neighborhood of such a point, appreciable fluid velocity toward the droplet center arises, and this flow causes a decrease in the thickness of the film which then permits the rampart to be stable except at the droplet.

The stability of the rampart can be analyzed by a crude analogy with the calculations

of Rayleigh for the stability of a long, free cylinder of liquid. He found that all disturbances of any wave length parallel to the fluid cylinder were amplified, but that the wave length which is most rapidly amplified was given by

$$\frac{\lambda}{r} = 9.02, \tag{6.2}$$

where r is the radius of the fluid cylinder.

In our case, the characteristic dimension a of the fluid rampart can be found by striking a balance between surface tension forces roughly given by 2σ and gravitational

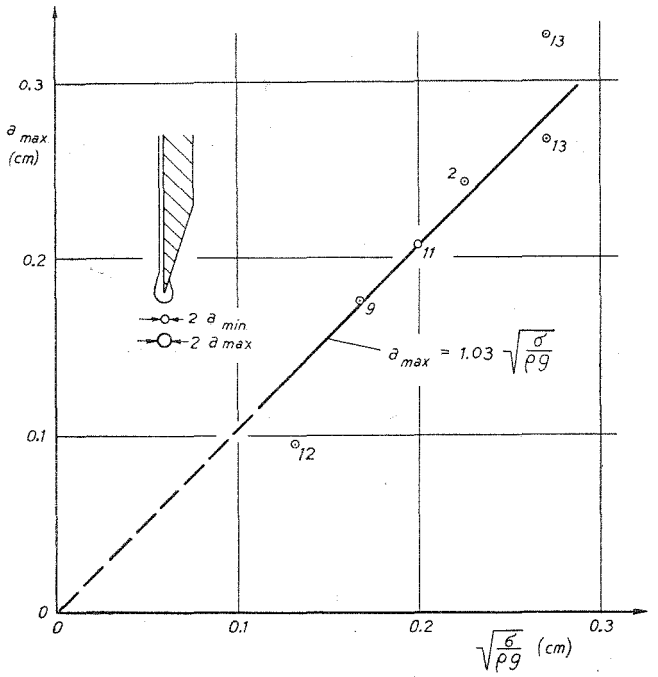

FIG. 10.

force $\pi a^2 \varrho g$. Thus, the characteristic radius a is roughly given by $\sqrt{\frac{2}{\pi}\frac{\sigma}{\varrho g}}$, and consequently,

$$\lambda = 9.02a = 7.2\sqrt{\frac{\sigma}{\varrho g}}. \tag{6.3}$$

The good agreement between this result and experiments (6.1) suggests that predominant here is the same process as is important for the free fluid cylinder.

The more precise theoretical investigations on instability of the interface between two liquids has been investigated by Bellman and Pennington. They found that for water, the critical wave-length is about $\lambda = 1.73$ cm which is in excellent agreement with the value obtained in this experiment in Fig. 8.

The formation of droplets at the edge of the plate is shown in Fig. 3d. Almost always, a large and a small droplet were formed in a single „drip" due to the breakup of the co-

lumn of liquid pulled off of the plate by gravitational forces. For the cases in which viscosity did not play a major role in the droplet formation, and when individual droplets rather than fluid streams left the lip of the plate, the radii of the droplets fell roughly into classes. If the radius of the larger is called a_{max}, then that of the smaller is about $^1/_3\, a_{max}$.

As in the previous case, we can study the mean radius of the large droplets by the dimensional analysis approach:

$$a_{max} = f(\sigma, \varrho, g) = C_2 \sqrt{\frac{\sigma}{\varrho g}}. \tag{6.4}$$

The values of a_{max} versus parameter $\sqrt{\sigma/\varrho g}$ are plotted in Fig. 10. The magnitude of constant C_2 can be determined from this graph as $C_2 = 1.03$. The relation between λ and a_{max} in this case is $x/a_{max} = 6.6$, whereas, in the case of a liquid jet, the value is roughly 5.

The ratio of gravity forces on the droplet to the surface tension force, defined as $2\pi a_{max}\sigma$, is

$$\frac{\frac{4}{3}\pi a_{max}^3 \varrho g}{2\pi a_{max}\sigma} = 0.7.$$

This value is in good agreement with values reported in the extensive literature on the subject of droplets, e.g. A.W. Adamson.

Acknowledgements. The authors wish to thank Dr. W. D. Rannie and Dr. F. E. Marble for entering discussions and making suggestions during this work.

References

[1] J. W. Strutt, (Lord Rayleigh), Phil. Mag., **30** (1890), 385.
[2] K. M. Dodd, *On the disintegration of water drops in an air stream*, J. Fluid Mech., **18** (1960), 175.
[3] A. A. Buzukow, *Razrushenie kapel' i struii zhidkosti vozdushnoi udarnoi volnoi*, Zhurnal prikladnoi mekhaniki i technicheskoi fiziki, 22 (1963), 154.
[4] G. Taylor, *The dynamics of thin sheets of fluid*, Proc. Roy. Soc. (London) A 253.
[5] R. Puzyrewski, S. Krzeczkowski, *Some Results of Investigations on Water-Film Break-up and Motion of Water Drops in Aerodynamics Wake*, Transactions of the Institute of Fluid Flow Machinery, No 29–31, 1966.
[6] Handbook of Chemistry and Physics, 33rd Edition, ed. by Charles D. Hodgman, Chemical Rubber Publ. Co., Cleveland, Ohio 1951–1952.
[7] V. G. Levich, *Physicochemical Hydrodynamics* trans. [from Russian], 1962.
[8] A. W. Adamson, *Physical Chemistry of Surfaces*, p. 25, Interscience Publishers, New York 1960.
[9] R. Bellmann and R. H. Pennigton, *Effects of surface tension and viscosity on Taylor instability*, Quart. Appl. Math., 2, **12** (1954).

INSTITUTE OF FLUID FLOW MACHINERY,
POLISH ACADEMY OF SCIENCES,
GDAŃSK, POLAND.
KÁRMÁN LABORATORY OF FLUID MECHANICS AND JET PROPULSION
CALIFORNIA INSTITUTE OF TECHNOLOGY, PASADENA,
CALIFORNIA USA.

Discussion

M. Z. KRZYWOBLOCKI (Michigan, USA)

It seems that in problem of the kind presented by author a tool based upon the dimensional analysis could be much stronger. It is possible that better equations, more appropriate for the problem in question could be derived directly from the theorems of the dimensional analysis as presented in the excellent work by SEDOV.